*36th EPS Conference on Plasma Phys. Sofia, June 29 - July 3, 2009 ECA Vol.**33E**, P-5.205 (2009)*

The observation of the small scale magnetic fluctuations with UHR cross-polarization scattering diagnostic at the FT-2 tokamak

A.B. Altukhov, L.A. Esipov, A.D. Gurchenko, E.Z. Gusakov, A.Yu. Stepanov

Ioffe Institute, St.Petersburg, Russia

Magnetic component of small-scale plasma turbulence can play an important role in electron transport disturbing the system of nested magnetic surfaces and causing huge energy losses along the field lines. The cross-polarization scattering (CPS) diagnostics utilizing microwave probing perpendicular to the tokamak magnetic field provides a unique opportunity for measuring relatively low magnetic turbulence level in the hot plasma core because intensive density fluctuations do not contribute to the CPS signal in this experimental geometry [1]. The scheme of the experiment utilizing the CPS effect in the Upper Hybrid Resonance (UHR) of the probing microwave was investigated at the FT-1 tokamak using the RADAR scheme [2] and last years developed at the FT-2 tokamak [3], where the signal originated in the UHR is separated using the radial correlation scheme. The potential advantages of CPS in UHR are particularly described in [3, 4]. In the present paper the detailed correlation measurements of the CPS signals performed at the FT-2 tokamak with two O-mode receiving antennas (one in equatorial plane and the second displaced at +15mm) are reported.

CPS scheme and diagnostics set up

The UHR CPS scheme has been assembled at the FT-2 tokamak (R=55 cm, a=7.9 cm, B_T=(1.8-2.2) T, I_p= (19-35) kA, $n_e(0)$= (0.5-6)×10^{13} cm^{-3}, T_e=(300-500) eV) where a double antenna set (*O*-mode for y_a = 0 mm and for y_a = 15 mm), shown in fig.1, was installed at the low magnetic field side in the same poloidal cross-section, but opposite to the movable focusing *X*-mode antennae, used for UHR microwave backscattering investigation [3]. The wave vectors satisfying the Bragg condition

$$\begin{pmatrix} k_{ir} \\ k_{i\theta} \end{pmatrix} + \begin{pmatrix} q_r \\ q_\theta \end{pmatrix} = \begin{pmatrix} k_{sr} \\ k_{s\theta} \end{pmatrix} \qquad (1)$$

for plasma fluctuation ($\vec{q}$) incident $\vec{k}_i$ and scattered $\vec{k}_s$ waves taking part in the CPS are shown in fig.2 for down shifted probing antennae position. Following [3] we supposed that the CPS signal is provided by the UHR region vicinity where the

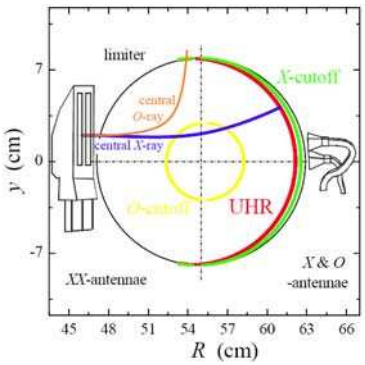

Fig. 1. *UHR cross section, Antennae set up.*

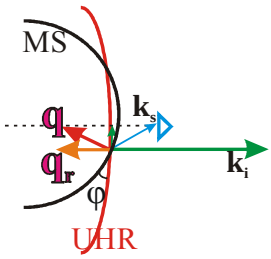

Fig. 2. *Wave vectors interaction scheme.*

scattering cross section is enhanced due to contribution of velocity fluctuations. In this region, according to [5] the radial and poloidal components of the probing wave vector satisfy the following relation $k_{i\theta} = k_{i\theta 0} + k_{ir} \cdot \sin\varphi$, here φ is an angle between magnetic and UHR surfaces at the scattering point. Assuming the main part of the signal to be provided by the probing beam centre and determining the wave vector $\vec{k}_s$ of the CPS wave received by the O-mode antenna from the ray tracing consideration we finally express the poloidal component of the fluctuation wave number in terms of the radial component:

$$q_\theta = k_{s\theta} - k_{i\theta} = k_{s\theta} - (k_{i\theta 0} + (k_{sr} - q_r) \cdot \sin\varphi) \qquad (2)$$

Using the fluctuation poloidal wave number (1) and the CPS signal frequency shift $\Omega = \omega_s - \omega_i$ we can obtain poloidal velocity of the fluctuations from the drift wave dispersion relation

$$2\pi f_D = \Omega = V_\theta \, q_\theta \qquad (3)$$

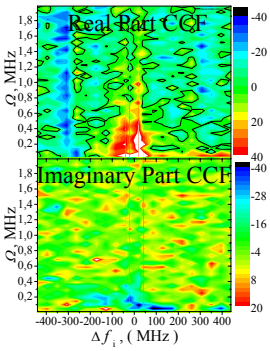

Fig. 3. *CCF.*

To resolve wave numbers of the fluctuations producing the CPS signal the correlative CPS technique is used. The plasma is probed simultaneously at two frequencies by *X*-mode wave in *V*-band from the high field side and *O*-mode signal was studied with new antennae sets for different exciting antenna vertical positions. One of generators probing at constant frequency (reference channel) defines the UHR position whereas the second generator frequency is changing on discharge to discharge basis. The scattering signals at both probing frequencies are stored by the data acquisition and used for computation of the cross-correlation function (CCF) presented in fig.3. The Fourier transformation of the CCF dependence on the channel frequency difference Δf_i proportional to the UHR spatial separation, gives the cross correlation spectrum (CCS), which is presented in fig.4. This CCS possessing clear sharp maximum at q_r=50-70 cm^{-1} and frequency $\Omega/2\pi$ = 100-200 kHz was obtained as a result of correlation measurements of the signal in ordinary polarization at low field side with both receiving and X-mode emitting antenna situated at +15 mm, whereas no signal allowing such a clear interpretation was observed by X-mode receiving antennae situated in the equatorial plane [3]. Besides the valuable signal the CCS shown in Fig.4, as well as that measured in [3], possess a well pronounced structure periodic in radial wave number *q* observable in wide frequency range exceeding 0.5 MHz

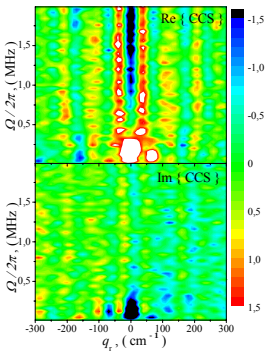

Fig. 4. *CCS.*

where no valuable signal was observed in the frequency spectra measurements. This parasitic effect was explained by strong correlation of signals at $\Delta f_i \approx \pm$ 300 MHz manifesting itself by pronounced narrow minimum CCF lines in fig.3, which convert into the periodic structure after Fourier transformation. To avoid these parasitic lines we performed the Fourier transformation of CCF in the narrower signal frequency range ($\Delta f_i <$ 300 MHz) improving the CCS reconstruction quality, but decreasing its wave number resolution. As it is seen in Fig.4, the CCS was obtained with a rather high error determined by the imaginary part value, which must be equal to zero in theory. Adjusting the phase of the CCF with the aim of the CCS imaginary part minimalization thus accounting for the asymmetry of the measurements scheme (detailed procedure was described in [6]) we have got spectra possessing the imaginary part decreased by a factor of two.

Experiments with O-mode receiving antenna in equatorial plane

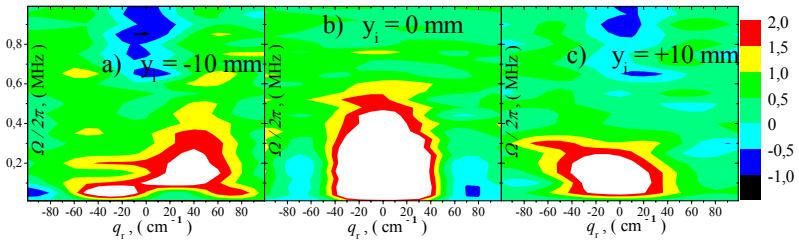

Fig. 5. *Real parts of the CCS for different probing antennae positions.*

The real parts of the CCS obtained with receiving antennae Os situated in the equatorial plane (0mm) are presented in fig.5 for three probing antennae positions (-10mm, 0mm, +10mm). In the case of non-shifted probing antenna the signal spectrum is symmetric concentrated near the zero wave number. It is most likely explained by the fact that the CPS in this geometry is produced by fluctuations possessing zero poloidal wave number. The vertical shift of the probing antenna by ±10mm results in spectrum asymmetry of opposite sign, as it is seen in Fig.4a and Fig.4c. This effect is easily interpreted in the framework of the Bragg resonance conditions (1). The visible asymmetry of Figures.4a-c is explained by slightly different vertical shift of the discharge in these experiments. The measurements described in the previous section have substantially improved the signal/noise ratio (SNR), however at frequencies lower than 100 kHz the spurious high amplitude signal related to the MHD activity still suppress the CPS signal reducing the SNR for all frequency range. Introducing high pass filters (f_c = 150 kHz) into the RF part of the receiving scheme resulting in MHD signal suppression, has improved the SNR in MF frequency range.

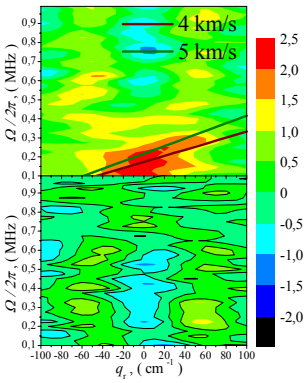

Fig. 6. *CCS with HP filters, y_i=-10mm*

Poloidal velocity estimations

The described improvement of the data processing procedure has allowed investigation of the turbulence dispersion relation using the CCS. As it is seen in Fig.6, the CPS is maximal along lines, which, according to (3), correspond to fluctuations possessing velocity in the range 4-5 km/sec. The velocity values calculated at one tokamak discharge regime at different experimental days are presented by different colors in fig.7. Temporal evolution of the toroidal field provided spatial scan in the minor radius from 4 cm to 6.5 cm with density variation about 10%. Supposing the signal to be generated due to the CPS off the magnetic fluctuations we may determine their wave number and frequency spectrum multiplying the CPS CCS of fig.6 by the CPS homodyne frequency spectrum and by the CPS efficiency, according to [4], proportional at high radial wave numbers to q^2. As it is seen in fig.8 the q-spectra for different frequencies of turbulence obey a knee-like double power law dependences with indexes equal to -2 and -5. The dependence plotted along the dispersion line of Fig.6 (violet triangles) also obeys the similar double power law. The q-spectrum decreases as q^{-2} for q less than 60 cm^{-1} and then rapidly decays q^{-5} at larger wave numbers. As it is seen in Fig.8, for fluctuations propagating in opposite direction the spectrum decay is slightly different.

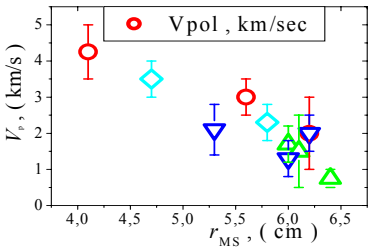

Fig. 7. *Red circle and dark blue triangles – Oi(-10mm)->Os(0mm) Light blue and green triangles - Oi(+10mm)->Os(0mm).*

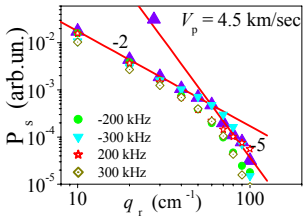

Fig. 8. *Magnetic fluctuations wave number spectra.*

Conclusion

In spite of relatively small value of the valuable CPS signal compared to the spectrum produced by MHD activity modulation of the spurious low power O-mode produced by the probing antenna, application of the correlation diagnostics made possible estimation of both spectrum and velocity of small scale magnetic field fluctuations. The obtained fluctuation poloidal velocity profile appears to be in reasonable agreement with those measured at FT-2 by several diagnostics that confirms the drift mode origin of the magnetic turbulence.

Financial support of RFBR grant 08-02-00989-a, 07-02-92162-CNRS_a and 09-02-09374-mob_z is acknowledged.

[1] Lehner T., Gresillon D., et al. Proc. 12th EPS Conf. on CFPP, Budapest, 1985, II, 664.
[2] D.G. Bulyiginskiy, A.D. Gurchenko, E.Z. Gusakov et al., Phys.Plasmas, 2001, 8, 2224.
[3] A.B. Altukhov, L.A. Esipov, A.D. Gurchenko et al., Proc 34 EPS Conf. on CFPP, 2007, V.31F, p-2.135.
[4] E.Z. Gusakov, Plasma Physics Reports, 2002, 28, 580.
[5] A.D. Gurchenko, E.Z. Gusakov, A.B. Altukhov, et al. Nucl. Fusion **47** (2007) 245–250.
[6] A.B. Altukhov, A.D. Gurchenko, E.Z. Gusakov, et al. Proc 35 EPS Conf. on CFPP, 2008, V.32D, D-5.011.